Hindawi Publishing Corporation
EURASIP Journal on Image and Video Processing
Volume 2007, Article ID 98181, 9 pages
doi:10.1155/2007/98181

*Research Article*

# Perceptual Image Representation

**Matei Mancas,[1] Bernard Gosselin,[1] and Benoît Macq[2]**

[1] *Théorie des Circuits et Traitement du Signal (TCTS) Lab, Faculté Polytechnique de Mons, 7000 Mons, Belgium*
[2] *Laboratoire de Télécommunications et Télédétection (TELE), Université Catholique de Louvain, 1348 Louvain-la-Neuve, Belgium*

Received 1 August 2006; Revised 8 March 2007; Accepted 2 July 2007

Recommended by Ling Guan

This paper describes a rarity-based visual attention model working on both still images and video sequences. Applications of this kind of models are numerous and we focus on a perceptual image representation which enhances the perceptually important areas and uses lower resolution for perceptually less important regions. Our aim is to provide an approximation of human perception by visualizing its gradual discovery of the visual environment. Comparisons with classical methods for visual attention show that the proposed algorithm is well adapted to anisotropic filtering purposes. Moreover, it has a high ability to preserve perceptually important areas as defects or abnormalities from an important loss of information. High accuracy on low-contrast defects and scalable real-time video compression may be some practical applications of the proposed image representation.

## 1. INTRODUCTION

The human visual system (HVS) is a topic of increasing importance in computer vision research since Hubel's work [1] and the comprehension of the basics of biological vision. Mimicking some of the processes done by our visual system may help to improve the current computer vision systems. Visual attention is part of a major task of the HVS, which is to extract relevant features from visual scenes in order to react in a relevant manner for our survival.

Several anisotropic filtering techniques are available for still images. These algorithms aim at preserving edges (considered as perceptually valuable) while they lowpass filter the rest of the image. These techniques are widely used in advanced image enhancement and sometimes in preprocessing of some segmentation steps for example. However, several visual attention (VA) models showed that edges were not the only areas in an image which are perceptually important. We propose here a novel and computationally efficient approach of visual attention for anisotropic filtering in both still images and video sequences. This global rarity-based approach better handles spatial and temporal texture and it performs accurate detection of low-contrast defects.

The general idea of our visual attention model is described in the next section. Sections 3 and 4 provide an adaptation of the rarity-based attention idea to still images and video sequences. Section 5 deals with an application of the proposed model to anisotropic filtering of both still images and videos. Finally, the last section will conclude the work and discuss our approach.

## 2. VISUAL ATTENTION

Treisman and Gelade [2] demonstrated that visual attention in still images can be divided into two distinct steps. The first one is a preattentive "parallel," unconscious, and fast process. The second one is an attentive conscious saccade-based image analysis which is a "serial" and slower process. Preattentive visual attention occurs faster than 200 milliseconds after viewing an image in the case of humans. For video sequences, preattentive vision seems to be more complex. Each new frame could be considered as a novel image, or the first 200 milliseconds of the video sequence should only be considered. Nevertheless in this latter case, what does the beginning of a video sequence mean in real life? If preattentive vision is an unconscious reflex which adapts itself to a time-evolving saliency map, it could be applied for each new fixation computation. This preattentive vision should compete in this case with higher-level feedback coming with the image understanding process: more an image makes sense, more the high-level feedback is important and vision becomes attentive. In the particular case of novel (never seen before) still images, there is no information for the first fixation, therefore the high-level feedback may be very low and the fixation preattentive; but in real life, the visual consciousness level depends on the degree of understanding of the environment from previous fixations.

As the definition of preattentive vision is unclear in real-life vision, we will use the term of low-level vision which highlights pop-out regions in a parallel way without comparing regions in the image. In this article, we will address this reflex low-level vision.

### *2.1. Biological background*

The superior colliculus (SC) is the brain structure which directly communicates with the eye motor command in charge of eye orientation. One of its tasks is to direct the eyes onto the "important" areas of the surrounding space. Studying the SC afferent and efferent paths can provide important clues about how biological systems classify scenes as interesting or not in a preattentive way.

There are two afferent pathways for the SC, one direct path from the retina and one indirect path crossing the lateral geniculate nucleus (LGN) and the primary cortex area V1 before coming back to the SC. There are also two efferent paths, one to the eye motor area of course, and the other one to the LGN. Studies on afferent SC pathways [3] showed that the direct path from the retina is responsible of spatial (W cells) and temporal (Y cells) analysis and the indirect pathway is mainly responsible of spatial and motion direction and certainly colour analysis. Both paths may be related to preattentive reflex attention but the indirect path also brings higher-level decisions responsible for attentive vision.

### *2.2. Attention modelling*

Many methods may be found in the literature about visual attention and image saliency. Some of them attempt to mimic the biological knowledge as Itti and Koch's (I&K) method [4]. They define a multiresolution- and multifeature-based system which models the visual search in primates. Le Meur et al. [5] suggested a global architecture close to I&K, but using a smart combination between the different feature maps. Instead of combining simply normalised feature maps, they use some coefficients which give more or less weight to the different features into the final saliency map. In these approaches, only local processes mimicking different cells are used.

Walker et al. [6], Mudge et al. [7], Stentiford [8], and Boiman and Irani [9] base their saliency maps on the idea that important areas are unusual in the image. The saliency of a configuration of pixels is inversely related to their occurrence frequency. These techniques use comparisons between neighbourhoods of different shapes and at different scales in order to assign an attention score to a region. Itti and Baldi [10] also published a probabilistic approach of surprise based on the Kullback-Leibler divergence also called "net surprisal." These methods have a more global approach and are based on the similarity quantification inside an image or a database.

We think that the local processing done by cells is somehow globally integrated (possibly inside the SC). Our definition will be based on the rarity concept which is necessarily global. We also think that our visual attention is not driven by a specific feature as some models could assess. Heterogeneous or homogeneous, dark or bright, symmetric or asymmetric, fast moving or slow moving objects can all attract our visual attention. The HVS is attracted by the features which are in minority in an image. That is why we can say that visual attention is based on the observation of things which are rare in a scene. Beyond the intuition that rarity is a concept of primary importance in computational attention, the work of Näätänen et al. [11] in 1972 on the auditory attention provided evidences that the evoked potential (electroencephalogram-based) has an improved negative response called mismatch negativity (MMN) when the subject was presented with rare stimuli than with frequent ones. Experiments were also made using the visual stimuli. Tales et al. [12] concluded to the existence of an MMN response to visual stimuli but the rare stimuli had a different complexity compared to the most frequent ones. Crottaz-Herbette led in her thesis [13] an experiment in the same conditions as Näätänen for auditory MMN in order to find out if a visual MMN really exists. The result was clearly positive with a high increase of the negativity of the evoked potential when seeing rare stimuli compared to the evoked potential when seeing frequent stimuli.

### *2.3. Rarity quantification*

A preattentive analysis is achieved by humans in less than 200 milliseconds; hence rarity quantification should be fast and simple. The most basic operation is to count similar areas (histogram) and provide higher scores to the rarest areas. Within the context of information theory, this approach is close to the self-information. Let us call $m_i$ a message containing an amount of information. This message is part of a message set $M$. A message self-information $I(m_i)$ is defined as:

$$I(m_i) = -\log(p(m_i)), \quad (1)$$

where $p(m_i)$ is the probability that a message is chosen from all possible choices in the message set $M$ (message occurrence likelihood). We obtain an attention map by replacing each message $m_i$ by its corresponding self-information $I(m_i)$. The self-information is also known to describe the amount of surprise of a message inside its message set [14] as it indicates how surprised we should be at receiving that message (the unit of self-information is the bit). We estimate $p(m_i)$ as:

$$p(m_i) = \frac{H(m_i)}{\mathrm{Card}(M)}, \quad (2)$$

where $H(m_i)$ is the value of the histogram $H$ for message $m_i$, and $\mathrm{Card}(M)$ is the cardinality of $M$. The quantification of the message set $M$ provides the sensitivity of $p(m_i)$: a smaller quantification value will let messages which are not exactly the same to be considered as similar.

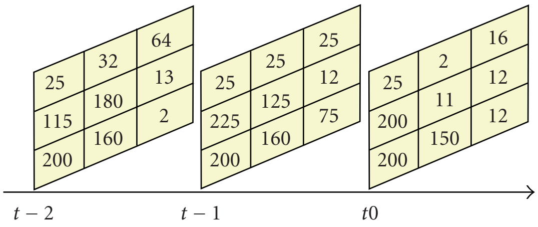

| | | |
|---|---|---|
| 25 | 32 | 64 |
| 115 | 180 | 13 |
| 200 | 160 | 2 |

| | | |
|---|---|---|
| 25 | 25 | 25 |
| 225 | 125 | 12 |
| 200 | 160 | 75 |

| | | |
|---|---|---|
| 25 | 2 | 16 |
| 200 | 11 | 12 |
| 200 | 150 | 12 |

Figure 1: Example of $m_i$ and $M$ on a three frame sequence of $3 \times 3$ images.

## 3. VISUAL ATTENTION FOR STILL IMAGES

In an image, we can consider in a first approximation that $m_i$ is the grey-level of a pixel at a given space location and $M$ is the entire image at a given time as shown in Figure 1. If we consider as a message the pixel with the coordinates $(2, 2, t_0)$, we have $m_i = 11$ and $M = \{25, 2, 16, 200, 11, 12, 200, 150, 12\}$.

The proposed model is global as the set $M$ is considered as the entire image and the probability of occurrence of each message is computed on the whole set. Nevertheless, comparing only isolated pixels is not efficient. In order to introduce a spatial relationship, areas surrounding each pixel should be considered.

Stanford [15] showed that the W-cells which are responsible of the spatial analysis inside the SC may be separated into two classes: the tonic W-cells (sustained response all over the stimulus) and the phasic W-cells (high responses at stimulus variations).

Our approach uses the mean and the variance of a pixel neighbourhood in order to describe its statistics and to model the action of tonic and phasic W-cells. We compute the local mean and variance on a $3 \times 3$ sliding window and our experience showed that this parameter is not of primary importance. To find similar pixel neighbourhoods, we count the neighbourhoods which have the same mean and variance (2). Contours and smaller areas get higher attention scores on the VA map (Figure 2, top row, second image). If we consider only local computations as, for example, the local standard deviation or the local entropy (Figure 2, top row, third and fourth image), contours are also highlighted but there are some differences like the camera fixation system or the cameraman's trousers. The local entropy seems to provide better results but the textured grass area has a too high score.

This difference is even more important on textured images. As it contains repeating patterns, its rarity score will be lower. More regular a texture is, less surprising it is and less important the attention score will be [16]. Local computations have a uniform high response for this textured image (Figure 2, bottom row, third and fourth image). In the case of our VA map (Figure 2, bottom row, second image), the response is important only for the white mark or the grey areas which are rare and which consequently attract human attention. Most of the vertical and horizontal separation lines between the bricks are also well highlighted. Achieved observations prove the importance of a global integration of the local processing made by the cells. Rarity or surprise which obviously attracts our attention cannot be computed only locally, but they need to be estimated on the whole image.

Moreover, Figure 3 compares I&K model to the proposed VA map for a visual inspection of an apple. The left image displays the original apple and the low-contrast defect contour in red. The I&K model does not manage to locate the defect even after more than 20 fixations and it focuses on the apple edges, whereas the proposed model (right image) provides to the defects the more important attention score after the apple edges. Even if for general purposes I&K model provides consistent results concerning saliency, our rarity-based model outperforms it in detecting abnormalities and defects especially in the case where these defects have a low contrast with their neighbourhood [17] and humans detect them using global rarity or strangeness in the image.

## 4. VISUAL ATTENTION FOR VIDEO SEQUENCES

Y cells, which are responsible for the motion analysis, have a high temporal resolution but a low spatial one [1]. Thus, the image spatial resolution is reduced and a $3 \times 3$ window mean filtering is applied on the resulting image. As Y cells are not sensitive to colour, only the luminance is used.

Message $m$ is here the grey-level of a pixel at a given spatial location and message set $M$ is the history of all grey-levels the pixel had over time. For example, the pixel with the coordinates $(2, 2, t_0)$ in Figure 1 has $m_i = 11$ and $M = \{180, 125, 11\}$.

However, if at each frame, the whole pixel history is needed, this may need huge size data to be stored. Hopefully, our ability to forget lets us specify a history size and to take into account only recent frames providing a limit to the set $M$.

As motion is generally rare in an image where most pixels are quite the same from one frame to another, moving objects will be naturally well highlighted. On the top of Figure 4, a video frame was annotated with two regions. Region 1 is a flickering light (regular time texture). The second region is a walking person. The middle row of Figure 4 displays a motion estimation map obtained by the subtraction of the current frame from a 200-frame-estimated background using a Gaussian model (GM) [18] and its thresholded map. The bottom row of Figure 4 displays our VA map computed on a 200-frame history and its thresholded map. The GM-based motion map and our VA map were both normalised and the same threshold was used in both cases. The two thresholded maps show that the region 2 is detected by both approaches.

Our model seems to detect more largely the walking person which is underestimated by the GM method, but it also detects a little part of its shadow. The most noticeable difference is in the region 1. Our VA model awards little attention score to the flickering light as it has a higher frequency and thus is a less rare event.

Figure 5 provides the results on another video sequence. Both methods correctly detected regions 1 and 2 (a moving car and a walking person). However, our method reacted with a very low attention score on region 3 (a tree moving because of the wind). The flickering light and the moving tree are well highlighted at the beginning of the video sequences

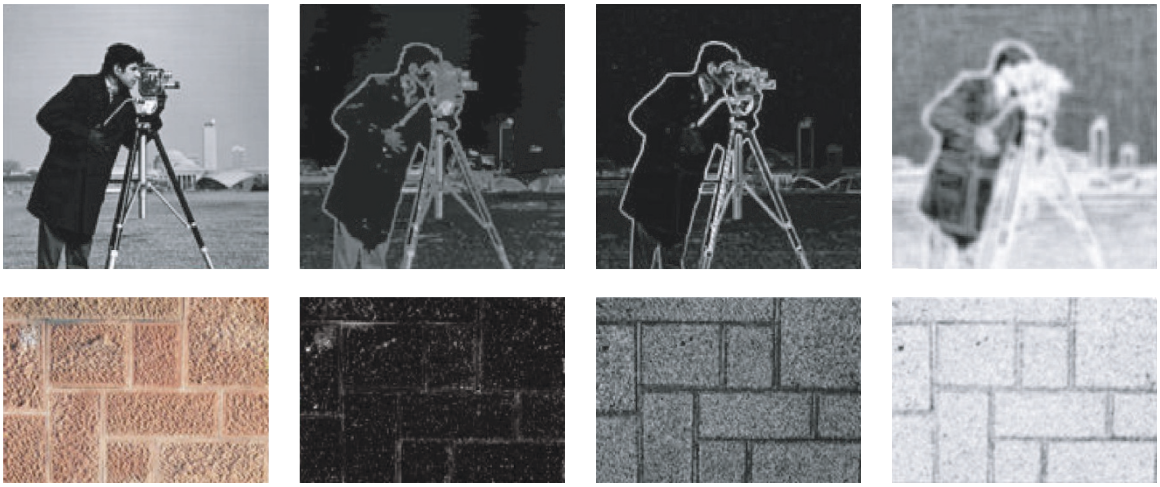

Figure 2: Left to right: initial image, proposed VA model, local standard deviation, local entropy.

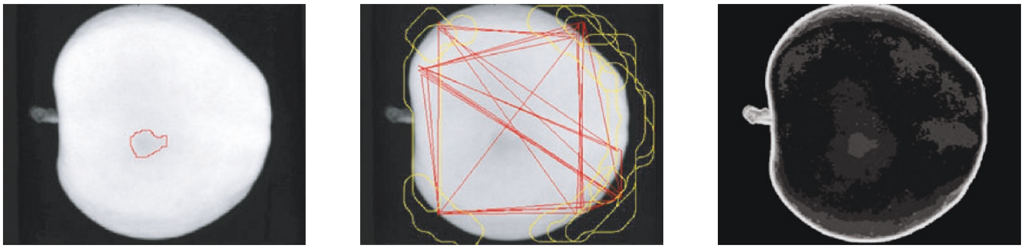

Figure 3: Left to right: original annotated defected apple, saccades and fixations in I&K, proposed VA map.

while the memory did not record enough events to see them as less rare, but after 200 frames, the attention score of these two events naturally decreases without the need of any high-level information or inhibition. As the attention map is here only computed in parallel across the visual field and no serial region computation is required, this is a low-level and reflex process. These two examples show that the same behaviour is obtained for temporal or spatial attention: textures, in space or in time, are considered as less important areas because of the global integration of information in space or in time.

## 5. APPLICATION: ANISOTROPIC IMAGE REPRESENTATION

### *5.1. An attention-based anisotropic filtering framework*

Unlike digital cameras and their uniform sampling acquisition system, humans do not see the world uniformly. The retina receptors are not equally dispatched on its surface, but they are concentrated around the centre of the optical axis in a place called fovea [1]. The image resolution exponentially decreases from the fovea to the retina periphery. The brain gets information about the visual environment by registering several views acquired while the eye fixates some "interesting points."

Computationally, these interesting points may be considered as the most highlighted areas of the VA map, thus the most salient regions in the image. While the eye fixates the highest-level attention areas, the resolution of the other areas dramatically decreases when going further and further from the fixations. The proposed perception of the visual environment is based on the fact that a mean observer will fixate the higher attention level areas and only then he will have a look at the others.

To mimic this perceptual behaviour, the VA map is first separated into 10 areas (10 is experimentally chosen) sorted by level of saliency. A decreasing resolution function ($1/x$ like) which is quite well correlated with the distribution of the cone cells in the retina is used. To decrease the resolution, a simple idea is to use lowpass filters with an increasing kernel size from the unfiltered most salient areas to the most filtered and least salient areas. The kernel size $K$ is defined as

$$K = \alpha + \beta\left(1 - \frac{1}{x}\right). \tag{3}$$

The variable $x$ represents the distance from the fovea. Here, $x$ is a vector with a range going from 1 to 10 as 10 importance levels were defined. A parameter $\beta$ provides control on the anisotropic image representation: more important $\beta$ is, more the kernel size increases faster and the image resolution decreases faster from the most salient to the least salient regions.

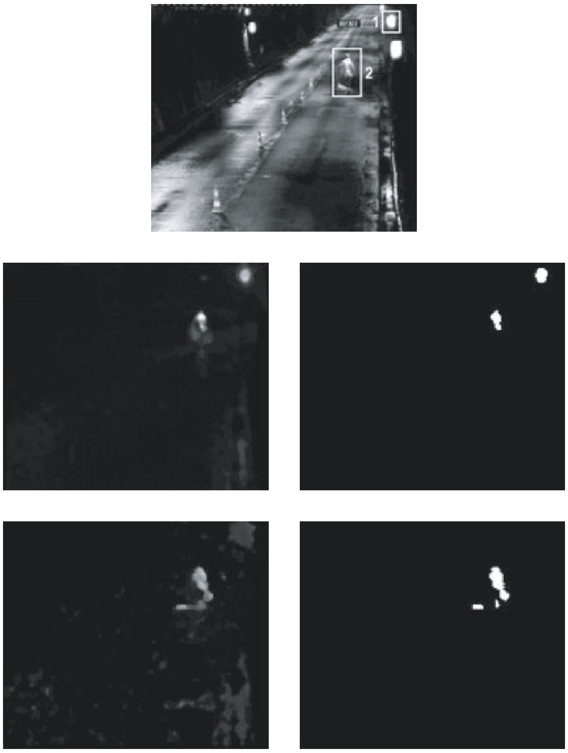

Figure 4: Annotated frame on top. Middle row: GM-based motion estimation map and thresholded map, Bottom row: our VA map and thresholded map.

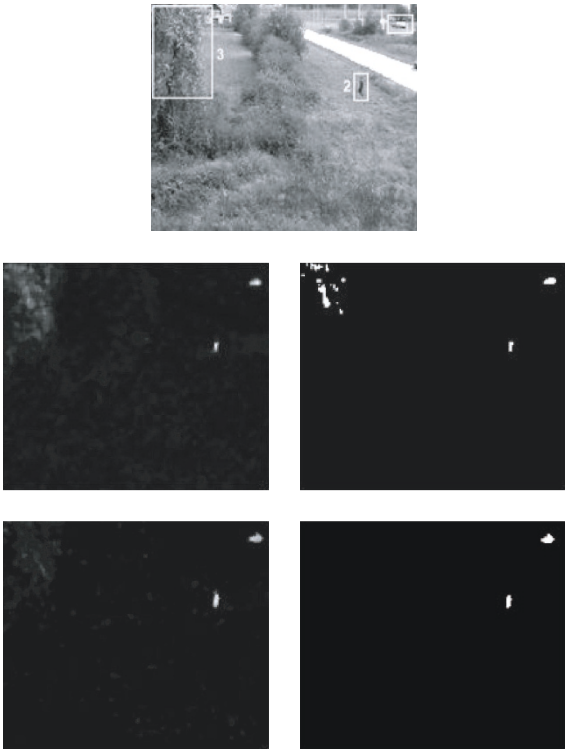

Figure 5: Annotated frame on top. Middle row: GM-based motion estimation map and thresholded map, Bottom row: our VA map and thresholded map.

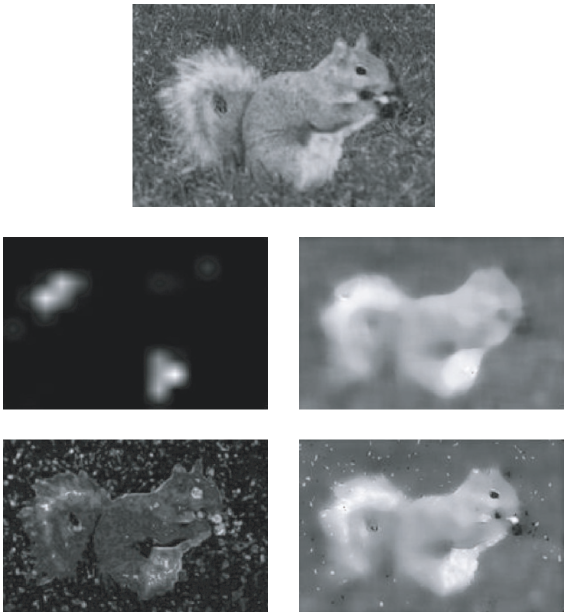

Figure 6: Left: original image, top row: I&K saliency map and corresponding anisotropic filtering ($\beta = 23$, $\alpha = 0$, OT $= 0$), Bottom row: our VA map and corresponding anisotropic filtering ($\beta = 23$, $\alpha = 0$, OT $= 0$).

The parameter $\alpha$ can optionally be used to control the kernel size of the filtering ($K$) for the most salient regions. The default value is "0" which means that the most salient areas from an image are not filtered at all. Nevertheless, in some applications (e.g., high frequency noise spreads on the entire image) one may want to filter with a certain kernel size even the most important areas.

Finally, a parameter called "observation time" (OT) is also added to the algorithm. When OT $= 0$, the image is visualised as previously described by keeping a good resolution only to the most salient regions. More OT increases, more we model the fact that a viewer has more time to observe the scene, hence after visualizing the most salient areas, he will also have a look at the least salient ones.

The filtering method used here to decrease the image resolution is a median filtering with increasing kernel sizes computed with (3). Nevertheless, several other lowpass filtering techniques with different kernel shapes could also be used. The used computational attention model is very important because the filtering result directly depends on the VA map and its characteristics. Saliency models which provide fuzzy saliency maps as I&K model are less convenient here: even if some important regions are well highlighted, many others are not taken into account and the filtering will not provide satisfying results on object boundaries. A comparison between anisotropic filtering using the proposed VA map and I&K saliency map is done in Figure 6. The visual attention model proposed by Stentiford could be more efficient in this case as it proved [19] its possibility in achieving still images coding. The problem is that there is no generalization of this model to video sequences until now. Moreover, it is

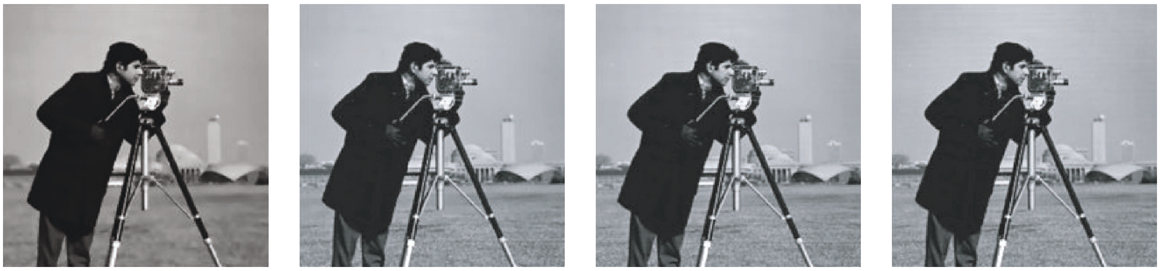

Figure 7: Anisotropic filtering ($\beta = 8$, $\alpha = 0$) from left to right: OT = 0, OT = 2, OT = 4 and OT = 8.

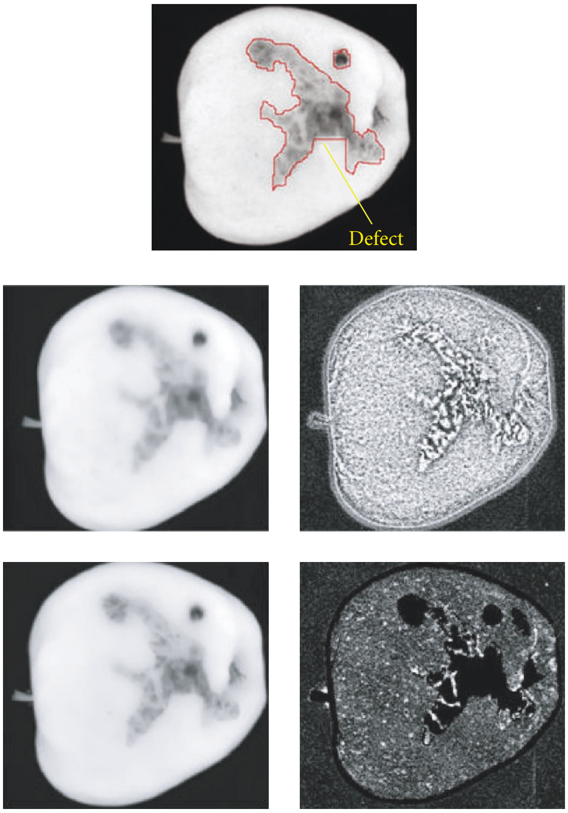

Figure 8: Top: the annotated original image, middle row: PM filtering and difference with the original, bottom row: proposed filtering and difference with the original.

difficult to compare several attention models as few of them are publicly available. Therefore, the proposed VA algorithm was chosen because it efficiently highlights the interesting areas and their edges which is important for filtering purposes. This method is also simple to implement and fast which is a critical point especially for video sequences filtering.

### 5.2. *Still images attention-based anisotropic filtering*

Figure 7 shows the cameraman image in an anisotropic representation ($\beta = 8$). When OT $=$ 0, only the very salient regions have a high resolution, as the rest of the image was lowpassed. When OT increases, the image resolution is enhanced in more regions until a uniform high resolution.

If we compare the proposed anisotropic representation with a classical anisotropic filtering as the Perona and Malik (PM) diffusion algorithm [20], there is no significant difference on an image like the cameraman. An objective comparison between the different algorithms is difficult and depends on the application of interest. Some papers which compare anisotropic filtering techniques use as a comparison criterion the fact that a filtering technique is "good" if it preserves well the boundaries and provides sharper "objects" edges than the others using several sets of parameters [21]. Based on the sharpness of the edges for a set of natural scene images, the results of the presented algorithm appeared to be equivalent to those of the PM algorithm. Even if for general purpose images, the proposed algorithm has equivalent results with already existing algorithms, it brings improvements for some categories of still images.

Our algorithm leaves the important areas unfiltered while classical approaches may filter the image between the high gradients. This case may be seen in Figure 8. The defect on the apple has an important contrast, so both methods keep the defect edges quite well defined even if the proposed method seems more accurate; but inside the defect, some variations have less contrast, which lead to different results using the PM algorithm and the proposed one. While details inside the defect are lost using the PM diffusion, they remain intact when using the proposed anisotropic filtering. This fact can be verified by the difference between the filtered image and the original one. If both methods filter the healthy skin, the PM algorithm also filters the defect and looses plenty of information about it (middle row, last image). The proposed algorithm keeps the main information of the defect unfiltered (bottom row, last image) preserving its characteristics.

In medical imaging, abnormalities are usually rare; therefore, pathologies can be awarded with higher attention scores even if the overall contrast is poor. Figure 9 displays an axial neck CT-Scan image where the presence of a tumour is identified. After a small observation time (OT $=$ 1) the active area of a tumour becomes interesting, therefore it remains unfiltered (bottom row) while the surrounding muscles are heavily filtered. For the same result on the muscles, the PM diffusion will filter the active tumour and loose information about it (middle row, first image). If the tumour is preserved, the muscles are not filtered enough (middle row, last image).

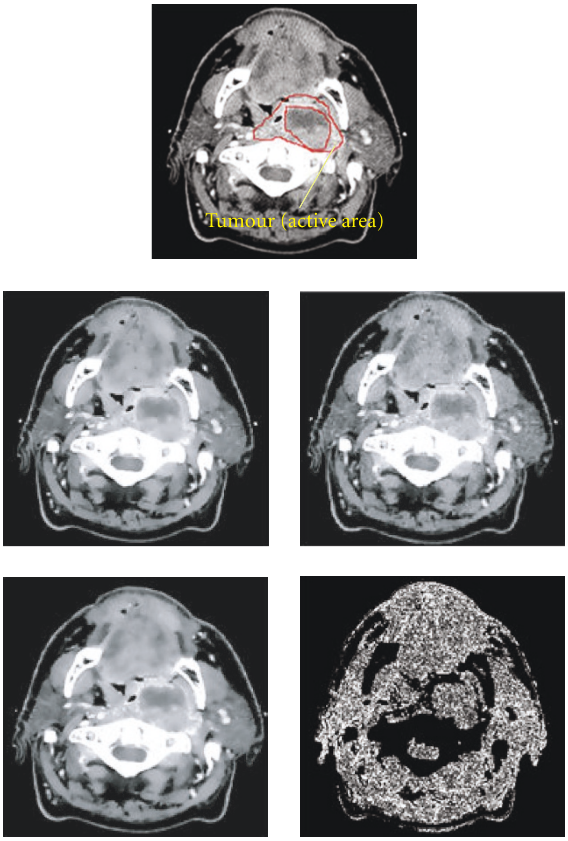

Figure 9: Top: the annotated original image, middle row: PM filtering (smooth muscles) and PM filtering (good quality tumour), bottom row: proposed filtering and difference with the original.

The ability to keep the entire region of interest unfiltered is an important advantage of the proposed method. Usually, full resolution is needed for regions of interest for further feature extraction in domains like image-based quality control or medical imaging.

### 5.3. *Video sequences attention-based anisotropic filtering*

Let us now generalise the image anisotropic representation to video sequences. The maximum operator is used to fuse the spatial and temporal saliency maps of a frame: humans react to the most important stimulus from all the saliency maps (Figure 10).

Figure 11 shows in each column for three different video sequences the evolution of the image resolution from a first frame to increasing OT values on the following frames. Humans first look at the moving regions, and then frame by frame they discover the rest of the image. Usually after a certain time, if the background is fixed, the observer will then focus only on the moving objects. If parts of the moving tree or flickering light have a good resolution even when OT = 0, this is not due to their temporal attention map (see Figure 4) but to their spatial saliency map.

The interest of the anisotropic filtering in video sequences is to enhance an adaptative coding or information transmission method. These methods aim at transmitting first important information with a small compression rate, and then the less important information with a higher compression rate. The proposed filtering technique is able to smoothen areas which are less important before the compression leading to a higher compression rate for the same quality factor.

Table 1 displays the sizes of the top frames in Figure 11 for the sequences S1, S2, and S3 and the different file sizes, function of the OT parameter after using a JPEG compression with a quality of 90. One can see that for low OT values, the images are naturally twice smaller than the original.

Even if the file size difference for OT = 5 or OT = 8 is less significant, the perceptual difference between the images is small and the difference of compression for a MJPEG video file (25 frames per second) could become significant. Moreover, by varying the OT value, the compression rate becomes scalable and it is able to adapt to the network in order to provide a realtime transmission, even if sometimes, details considered as less important are smoothed. The main information may remain unfiltered and realtime. For this scheme, classical MJPEG compression algorithm would remain unchanged: the only need is an anisotropic filtering before the transmission. Here, the transmission "intelligence" is not contained into the compression algorithm but in the preprocessing step.

## 6. CONCLUSION

We presented a rarity-based visual attention (VA) model working on both still images and video sequences. This model is a reflex one and it takes into account the whole image and not only local processing. Mathematically, the model is based on the self-information (1) which expresses how "surprising" information is and its results are close to the expected reaction of a human.

Comparisons were made between the spatial VA map, the gradient amplitude and the local entropy, showing some similarities but also fundamental differences connected to the global computation of our model versus local computations. As spatial textures are repeating patterns, their rarity and their saliency will be lower than the saliency of each of their isolated patterns. The proposed model was also compared with a reference publicly available algorithm: the I&K model. For the precise case of low-contrast defects, our VA model outperforms the I&K one.

The temporal VA map was compared to the classical GM background estimation using Gaussians to model pixel behaviours. Similar results were obtained for most movements, but again, we noticed differences concerning the temporal textures. When pixel values often repeat in time, the area saliency drops using our model. The GM-based background estimation will add the texture "mean" to the background and false detection or false alarms can be caused even by regular temporal textures as flickering lights or moving trees. Our model avoids most of these problems as it assumes that

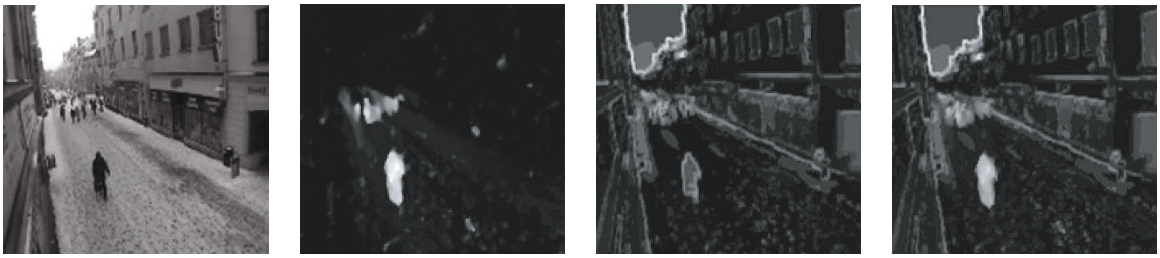

Figure 10: Left to right: the video frame, the temporal VA map, the spatial VA map and the final VA map.

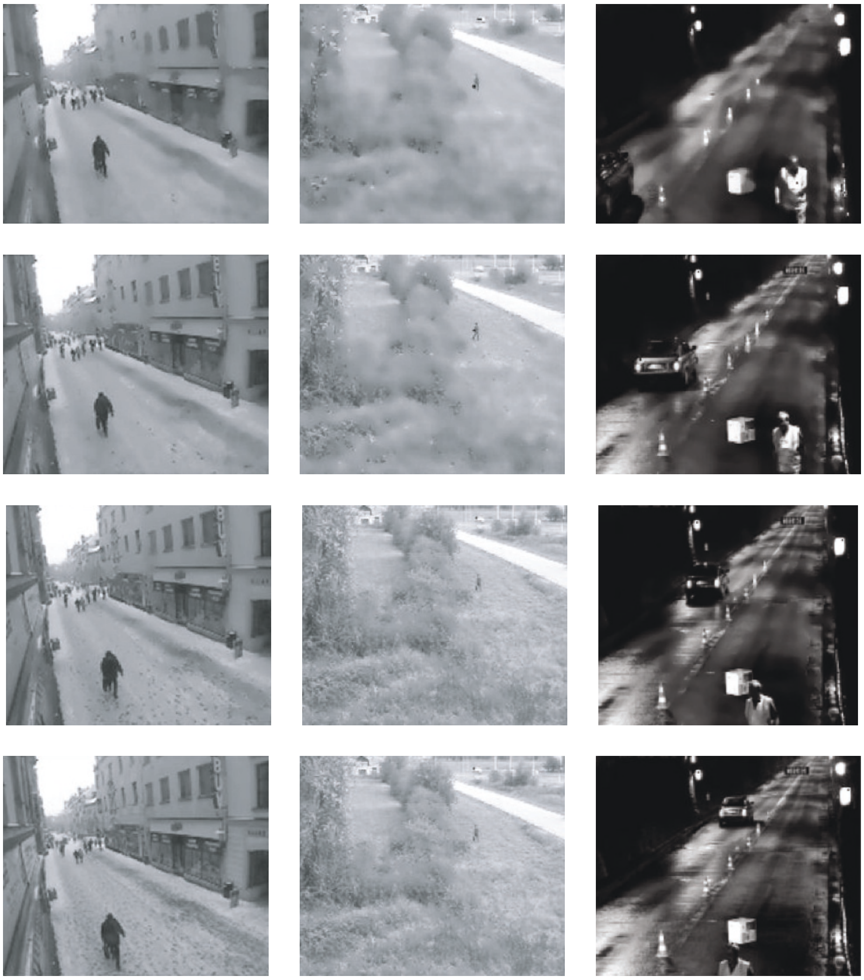

Figure 11: Top to bottom: anisotropic representation on several consecutive frames for sequences S1, S2, S3 ($\beta = 21$, $\alpha = 0$, OT $= 0, 2, 5, 8$ from top to bottom).

these temporal textures are not rare and allow low attention scores to them.

An anisotropic representation based on the retina properties was then provided for both still images and video sequences. The presented model is particularly well adapted to provide attention maps for filtering and coding as opposed with I&K model which provides fuzzy saliency maps difficult to use for this particular application. Comparisons with the classical Perona and Malik anisotropic filtering were made. Similar results were often obtained, however our method seems to provide smoother results. Moreover, as the anisotropic filtering is gradient-based, the behaviours of our image representation and the classical anisotropic filtering are very different when textures take an important place in the image. A medical imaging example and an apple defect example show that our image representation provides high resolution to high gradients but also to defects and abnormalities. This shows that our model is a first step into image

Table 1: JPEG quality 90 compression on original S1, S2, S3 top frames from Figure 11 and on filtered frames using the proposed perceptual representation at different OT values.

| OT | S1<br>(original: 6.39 KB) | S2<br>(original: 8.29 KB) | S3<br>(original: 7.47 KB) |
|---|---|---|---|
| 0 | 3.89 KB | 3.99 KB | 3.39 KB |
| 2 | 5.19 KB | 5.93 KB | 5.41 KB |
| 5 | 6.14 KB | 7.58 KB | 6.74 KB |
| 8 | 6.36 KB | 8.10 KB | 7.29 KB |

understanding and even at a low-level processing, important information is more accurately found than with local processing methods.

The perceptual video images representation that we provide seems to correspond to a human-like approach of our environment with high attention scores on moving objects, but also with a progressive discovery of the background. Examples on several video sequences show this evolution of image discovery and demonstrate the ability to provide higher compression rates for the same JPEG quality compression. Scalable video compression can thus be achieved by varying the OT parameter of the anisotropic filtering prior to the compression step.

Compared to other global attention models described in Section 2.2, our approach is much simpler and related to the information theory framework. It can be generalised from image to video and even to other signals like sound. Moreover, our model does not use multiresolution at this stage and it can be efficiently coded for real-time processing.

## ACKNOWLEDGMENT

The authors would like to thank the Multivision group of Multitel research centre, Belgium for the high quality and numerous video sequences they provided.

## REFERENCES

[1] D. H. Hubel, *Eye, Brain, and Vision*, Scientific American Library, no. 22, W. H. Freeman, New York, NY, USA, 1989.

[2] A. M. Treisman and G. Gelade, "A feature-integration theory of attention," *Cognitive Psychology*, vol. 12, no. 1, pp. 97–136, 1980.

[3] J. W. Crabtree, P. D. Spear, M. A. McCall, K. R. Jones, and S. E. Kornguth, "Contributions of Y- and W-cell pathways to response properties of cat superior colliculus neurons: comparison of antibody- and deprivation-induced alterations," *Journal of Neurophysiology*, vol. 56, no. 4, pp. 1157–1173, 1986.

[4] L. Itti and C. Koch, "A saliency-based search mechanism for overt and covert shifts of visual attention," *Vision Research*, vol. 40, no. 10–12, pp. 1489–1506, 2000.

[5] O. Le Meur, P. Le Callet, D. Barba, and D. Thoreau, "A coherent computational approach to model bottom-up visual attention," *IEEE Transactions on Pattern Analysis and Machine Intelligence*, vol. 28, no. 5, pp. 802–817, 2006.

[6] K. N. Walker, T. F. Cootes, and C. J. Taylor, "Locating salient object features," in *Proceedings of the 9th British Machine Vision Conference (BMVC '98)*, vol. 2, pp. 557–566, Southampton, UK, September 1998.

[7] T. N. Mudge, J. L. Turney, and R. A. Volz, "Automatic generation of salient features for the recognition of partially occluded parts," *Robotica*, vol. 5, no. 2, pp. 117–127, 1987.

[8] F. W. M. Stentiford, "An estimator for visual attention through competitive novelty with application to image compression," in *Proceedings of the 22nd Picture Coding Symposium (PCS '01)*, pp. 101–104, Seoul, Korea, April 2001.

[9] O. Boiman and M. Irani, "Detecting irregularities in images and in video," in *Proceedings of the 10th IEEE International Conference on Computer Vision (ICCV '05)*, vol. 1, pp. 462–469, Beijing, China, October 2005.

[10] L. Itti and P. Baldi, "A principled approach to detecting surprising events in video," in *Proceedings of IEEE Computer Society Conference on Computer Vision and Pattern Recognition (CVPR '05)*, vol. 1, pp. 631–637, San Diego, Calif, USA, June 2005.

[11] R. Näätänen, A. W. K. Gaillard, and S. Mäntysalo, "Early selective-attention effect on evoked potential reinterpreted," *Acta Psychologica*, vol. 42, no. 4, pp. 313–329, 1978.

[12] A. Tales, P. Newton, T. Troscianko, and S. Butler, "Mismatch negativity in the visual modality," *NeuroReport*, vol. 10, no. 16, pp. 3363–3367, 1999.

[13] S. Crottaz-Herbette, "Attention spatiale auditive et visuelle chez des patients héminégligents et des sujets normaux: étude clinique, comportementale et électrophysiologique," M.S. thesis, University of Geneva, Geneva, Switzerland, 2001.

[14] M. Tribus, *Thermodynamics and Thermostatics: An Introduction to Energy, Information and States of Matter, with Engineering Applications*, D. Van Nostrand, New York, NY, USA, 1961.

[15] L. R. Stanford, "W-cells in the cat retina: correlated morphological and physiological evidence for two distinct classes," *Journal of Neurophysiology*, vol. 57, no. 1, pp. 218–244, 1987.

[16] M. Mancas, C. Mancas-Thillou, B. Gosselin, and B. Macq, "A rarity-based visual attention map: application to texture description," in *Proceedings of IEEE International Conference on Image (ICIP '06)*, pp. 445–448, San Antonio, Tex, USA, September 2006.

[17] M. Mancas, B. Unay, B. Gosselin, and D. Macq, "Computational attention for defect localisation," in *Proceedings of ICVS Workshop on Computational Attention & Applications (WCAA '07)*, Bielefeld, Germany, March 2007.

[18] C. R. Wren, A. Azarbayejani, T. Darrell, and A. P. Pentland, "Pfinder: real-time tracking of the human body," *IEEE Transactions on Pattern Analysis and Machine Intelligence*, vol. 19, no. 7, pp. 780–785, 1997.

[19] A. P. Bradley and F. W. M. Stentiford, "JPEG 2000 and region of interest coding," in *Digital Image Computing: Techniques and Applications (DICTA '02)*, pp. 303–308, Melbourne, Australia, January 2002.

[20] P. Perona and J. Malik, "Scale-space and edge detection using anisotropic diffusion," *IEEE Transactions on Pattern Analysis and Machine Intelligence*, vol. 12, no. 7, pp. 629–639, 1990.

[21] D. Barash and D. Comaniciu, "A common framework for nonlinear diffusion, adaptive smoothing, bilateral filtering and mean shift," *Image and Vision Computing*, vol. 22, no. 1, pp. 73–81, 2004.